J Mater Sci: Mater Electron (2015) 26:9789–9794
DOI 10.1007/s10854-015-3650-7

Facile one-step synthesis of PI/Fe_3O_4 composite microspheres from poly(amic acid) triethylamine salts and Fe(III) ion

Haoran Zhou[1] · Weimiao Yu[1] · Chunyan Qu[2,3] · Changwei Liu[2] · Dezhi Wang[2]

Received: 10 July 2015 / Accepted: 16 August 2015 / Published online: 25 August 2015

Abstract Polyimide/magnetite composite microspheres were successfully prepared from poly(amic acid) triethylamine salts and Fe(III) ion via a simple one-step solvothermal process. The formation mechanism of the composite microspheres was explored. The morphology and the structure of the samples were characterized. It was found that polyimide has successfully coated on the surface of the magnetite microspheres and penetrated throughout the crystals via an assembly process. And the magnetic and thermal properties were measured, the results showing that composite microspheres have excellent thermal stabilities and the saturation magnetization is 35.29 emu/g with PI content of 60 wt%.

1 Introduction

Magnetite (Fe_3O_4) is one of the oldest known magnetic materials, and recently it has been extensively studied in particular due to its high saturation magnetization, biocompatibility and low toxicity properties [1–4]. Because of this, Fe_3O_4 is widely used in catalysis [5], wave absorption [6, 7], environmental remediation [8], biotechnology/biomedicine [9, 10] and magnetic resonance imaging [11, 12]. However, naked magnetite nanoparticles are chemically highly active, and are easily oxidized in air, resulting generally in loss of magnetism and dispersibility. Constructed a core–shell structural magnetite hybrid nanoparticles are exceptionally promising protection strategy, these shell materials including polymers [13, 14], silica [15, 16], carbon [17, 18] and precious metals [19]. The core–shell structures with magnetite nanoparticles as the core with covalently grafted organic polymers as the shell has been studied extensively because of which has specific functions, such as biocompatibility and biological activity [20, 21]. Arias et al. [22] have prepared Fe_3O_4/chitosan nanocomposite for magnetic drug targeting to cancer. Lan et al. [23] have synthesized Fe_3O_4/poly(methyl methacrylate) composite nanospheres via a facile miniemulsion polymerization, as a nanoplatform for multimodal protein separation. However, there is a drawback of polymer-coated magnetite nanoparticles is the relatively low intrinsic stability of the coating at higher temperature [24]. Among various polymers, polyimide (PI) has outstanding performance with excellent thermal stabilities, excellent mechanical and electrical properties, as well as superior chemical resistance. It has been used in many different applications [25–27]. Therefore, covering magnetite microspheres with polyimide may improve their thermal stability and dispersibility. However, to the best of our knowledge, there are no reports in the literature of the one-step preparation of PI/Fe_3O_4 composite microspheres from iron and polyimide precursors.

In this paper, we present a facile one-step solvothermal method for preparation of PI/Fe_3O_4 composite microspheres using poly(amic acid) triethylamine salts (PAAS) and ferric chloride hexahydrate ($FeCl_3 \cdot 6H_2O$) as raw materials. There was no additional precipitating agent

✉ Haoran Zhou
zhouhaoran2013@163.com

✉ Changwei Liu
ailp_liuchangwei@sina.com

[1] School of Material Science and Engineering, Harbin University of Science and Technology, Harbin 150000, China

[2] Institute of Petrochemistry, Heilongjiang Academy of Science, Harbin 150000, China

[3] Institude of Advanced Technology, Heilongjiang Academy of Sciences, Harbin 150000, China

added during the reaction, except for the triethylamine, generated from the high temperature thermal cyclization of the polyimide structure. Detailed characterization of the products was carried out in order to demonstrate the feasibility of this method for the production of PI/Fe_3O_4 composite microspheres. The thermal stabilities and magnetic properties of PI/Fe_3O_4 composite microspheres were studied by thermo gravimetric analyses and vibrating sample magnetometer, respectively.

2 Experimental

2.1 Materials

N,*N*-dimethylacetamide (DMAc), ethylene glycol (EG), triethyleamine (TEA) were purchased from Tianjin Fuyu Fine Chemical Co., Ltd. Pyromellitic dianhydride (PMDA) was purchased from Sinopharm chemical Reagent Co., Ltd. 3,4′-oxydianline(3,4′-ODA) was obtained from Changzhou sunlight chemical Co., Ltd. Ferric chloride hexahydrate ($FeCl_3{\cdot}6H_2O$) was obtained from Tianjin Yuanli Chemical Co., Ltd. All the reagents were of analytical grade and used as received without purification.

2.2 Synthesis of PI/Fe_3O_4 composite microspheres

The precursor of polyimide, poly(amic acid) triethylamine salt, was synthesized by PMDA, 3,4′-ODA and TEA monomers with a molar ratio of PMDA/3,4′-ODA/TEA = 1:1:2 [28]. 10.0 g 3,4′-ODA and 125 ml DMAc were added to a 250 ml three-neck round-bottom flask fitted with a mechanical stirrer. Once the 3,4′-ODA had dissolved completely, an equivalent molar quantity (10.9 g) of PMDA was added, and the mixture was stirred for 4 h. After creating the PAA solution, 10.1 g of TEA at a PAA–TEA molar ratio of 1:2 was added into PAA solution and the mixture was stirred for 4 h. Finally, the PAAS solution was obtained with mass fraction of 20 %.

20.0 g of PAAS solution was added to the 50 ml mixed solvent of DMAc and EG with a volume ratio of 1:1 and stirred until PAAS completely dissolved, then 1.6 g $FeCl_3{\cdot}6H_2O$ was added to this solution to stirred for 1 h to get an homogeneous solution. Then the mixture was transferred to a 100 ml Teflon-lined autoclave for treatment at 200 °C for 8 h. The products were extracted with the help of a permanent magnet and washed with deionized water and acetone three times, and then dried in a vacuum oven at 75 °C for 6 h. The pure Fe_3O_4 microspheres were synthesized by the solvothermal method using mixed solvents and triethylamine as a precipitant.

2.3 Characterization

Scanning electron microscopy (SEM) images were obtained with a Quanta 200 microscope with an accelerating voltage of 20 kV. Transmission electron microscopy (TEM) images were carried out on a JEM-2100 transmission electron microscope with an accelerating voltage of 200 kV. X-ray diffraction (XRD) analysis was performed using a Y500 diffractometer by use of a Cu Kα source, with a step of 0.02° and a scan range between 10° and 90°. IR spectra (IR) were recorded on a Bruker Equinox 55 Fourier transform IR spectrometer, samples were ground and mixed with KBr and then pressed into plates and the range of scanning wave numbers was 400–4000 cm^{-1}. The thermo gravimetric analyses (TGA) were performed using a Pyris 6 TGA operated under an air atmosphere at a heating rate of 10 °C/min. Magnetic measurements were studied using a vibrating sample magnetometer (VSM) at room temperature.

3 Results and discussion

A possible mechanism for the synthesis of PI/Fe_3O_4 composite microspheres is illustrated in Scheme 1. Iron(III) ions are first attracted to the mainchains of PAAS through the complexation effects. As the temperature increases, triethelamine gets moved out from PAAS to the solution, which causes the increase of pH. Finally, iron oxide is precipitated under the weakly alkaline condition, where ethylene glycol serves as a reductant to favor the formation of Fe_3O_4 instead of Fe_2O_3 at a high temperature. Meanwhile, the formed intermediate, PAA, was imidized immediately, and it deposited precipitated on the nanocrystal grains to form the composite microspheres.

Figure 1 shows the SEM and TEM images of the prepared microspheres. As can be seen in Fig. 1, by comparing pure Fe_3O_4 microspheres (Fig. 1a) and PI/Fe_3O_4 composite microspheres (Fig. 1b), the rough surface and larger diameter (approx. 1 μm) of the composite microspheres may be due to the polyimide covering the surface of Fe_3O_4 microspheres, its penetration into the magnetic particles and formation of the core–shell magnetic polymers. The TEM images (Fig. 1c, d) also indicate that the Fe_3O_4 microspheres have been successfully coated with PI. The dark areas of the core consist of lots of magnetite crystal grains, in contrast, the polyimide, showing up as the light areas in the TEM images. Coats not only the surface of the particles, but each individual crystal grain we can see from Fig. 1d. And we can see from the Fig. 2c the crystal grain is fixed with the angle of towards the core this may due to the PI backbones have a directional effect on the

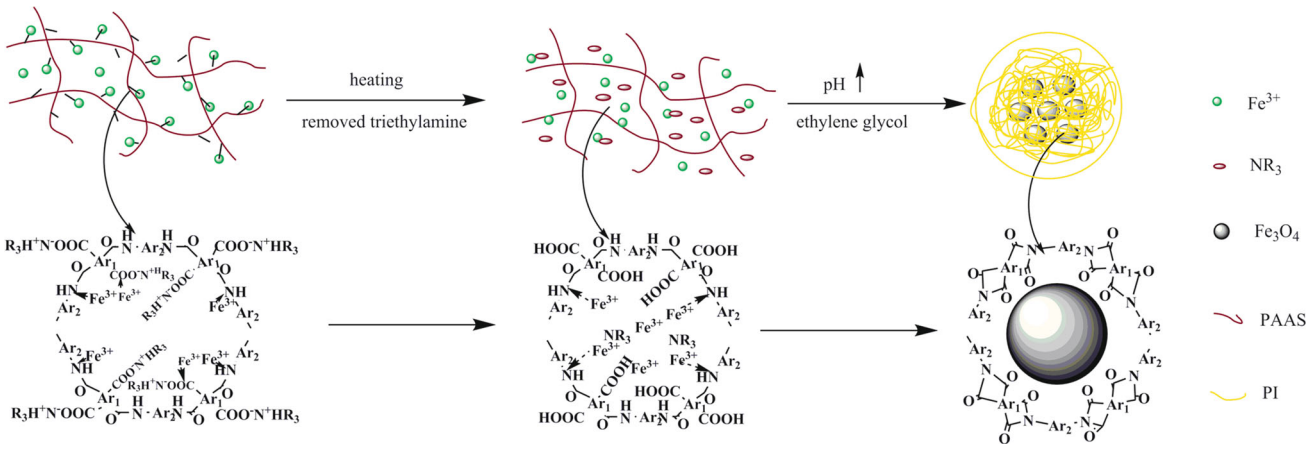

Scheme 1 Formation processes of PI/Fe_3O_4 composites microspheres

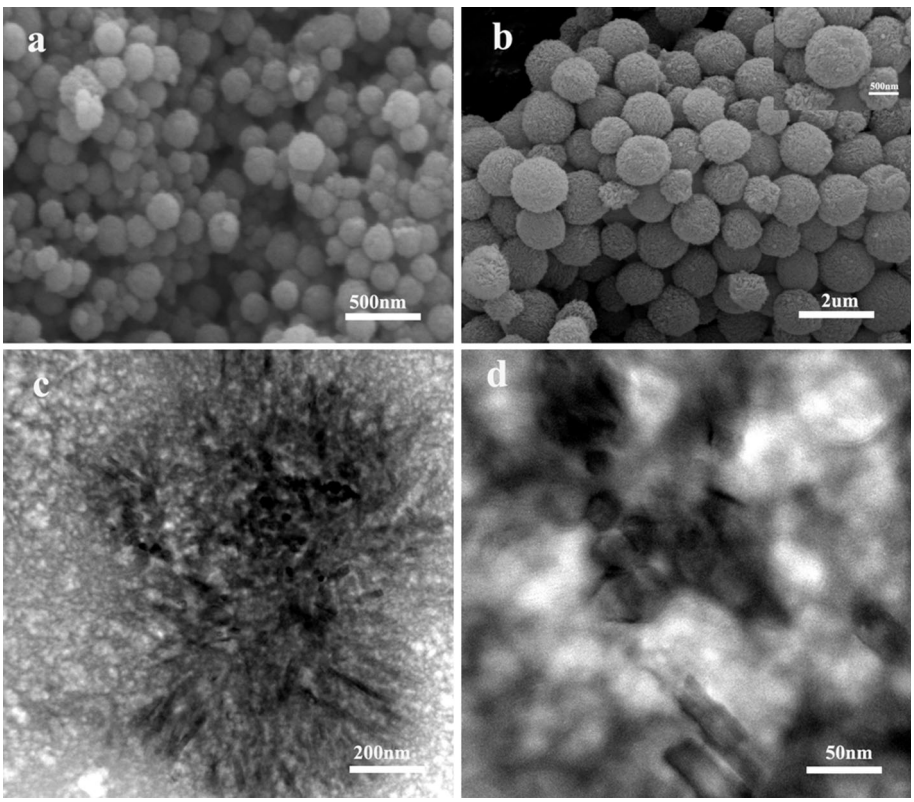

Fig. 1 SEM images of **a** Fe_3O_4 microspheres and **b** PI/Fe_3O_4 microspheres; **c**, **d** TEM images of PI/Fe_3O_4 microspheres

crystal growth due to iron(III) ions complexed to the chains of PAAS.

The crystalline structures of Fe_3O_4 and PI/Fe_3O_4 composite microspheres were identified and XRD patterns are shown in Fig. 2. For the pure Fe_3O_4 sample (Fig. 2a), there are five clear diffraction peaks ($2\theta = 30.12°$, 35.48°, 43.12°, 57.02° and 62.62°), corresponding to indices (220), (311), (400), (511) and (440), which match well with the magnetite (the JCPDS, No. 19-0629). These five characteristic peaks can also be observed in the PI/Fe_3O_4 composite microspheres XRD pattern (Fig. 2b), which due to the polyimide coated onto the surface of Fe_3O_4 does not change the crystal type. But the diffraction peaks are weaker and broader, which indicates the formation of an amorphous structure due to PI being deposited on the Fe_3O_4 microspheres. Also according to this result, the averages crystalline size of Fe_3O_4 and PI/Fe_3O_4 composite microspheres is 34.27 and 18.09 nm, respectively, as estimated from the (311) diffraction peak by the Scherrer equation [29, 30].This

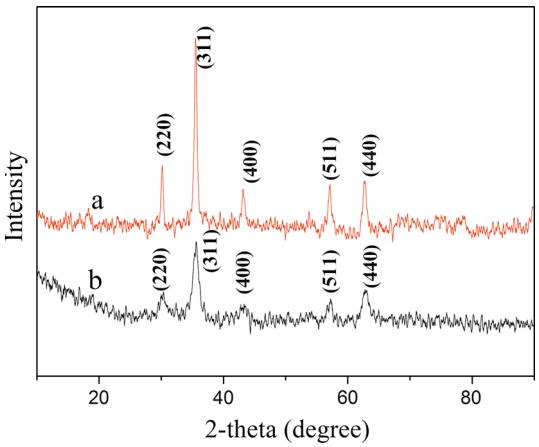

Fig. 2 XRD patterns of (*a*) pure Fe_3O_4 sample and (*b*) PI/Fe_3O_4 sample

shows that PAAS is not only used as a coating material but also as a dispersant.

Figure 3 shows the IR spectra of pure Fe_3O_4 and PI/Fe_3O_4 composite microspheres. In the spectrum of pure Fe_3O_4 (Fig. 3a), the strong absorption at 591 cm^{-1} represents a typical peak of Fe_3O_4, which is assigned to the characteristic band of the Fe–O group. The characteristic absorption peaks at 1776 (C=O imide asymmetrical), 1713 (symmetrical stretching), 1360 (C–N stretching) and 721 cm^{-1} (C–N bending) corresponds to polyimide can be seen from curve of the PI/Fe_3O_4 composite microspheres (Fig. 3b), which reveals that the imidization reaction of the polyimide is completely. And the typical peaks of Fe_3O_4 at 591 cm^{-1} also can be found at the curve of the PI/Fe_3O_4 composite microspheres, which indicates that PI had been spontaneously deposited onto the Fe_3O_4 microspheres.

The TGA curves of the pure Fe_3O_4 microspheres, the PI/Fe_3O_4 composite microspheres and the PI powder are shown in Fig. 4. The weight increases between 220 and

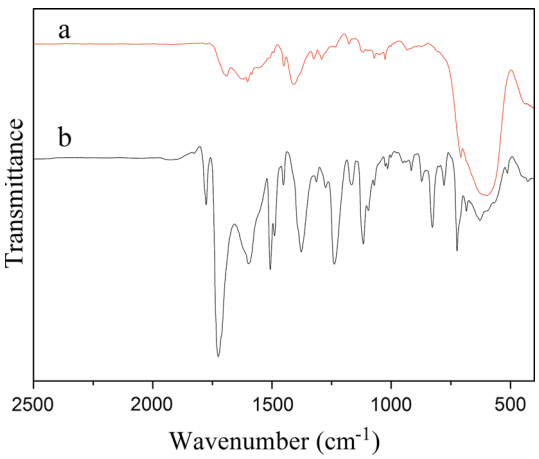

Fig. 3 IR spectra of (*a*) pure Fe_3O_4 sample and (*b*) PI/Fe_3O_4 sample

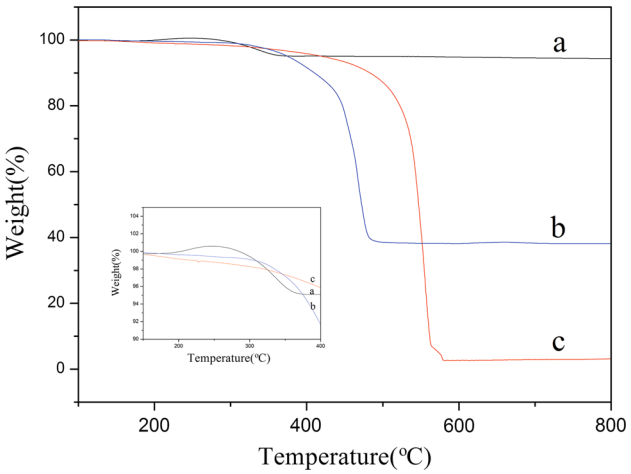

Fig. 4 TGA curves of (*a*) pure Fe_3O_4, (*b*) PI/Fe_3O_4 composite microspheres and (*c*) pure PI powder

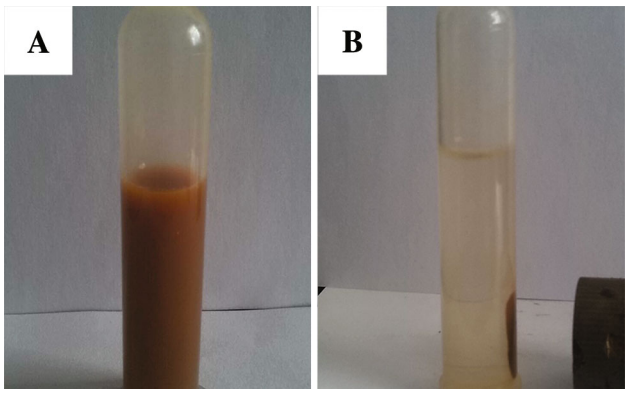

Fig. 5 Photograph of PI/Fe_3O_4 composite microspheres before (**a**) and after (**b**) application of a magnetic field

270 °C in the curve of pure Fe_3O_4 (Fig. 4a), due to the oxidization of magnetite in air atmospheres. However, this phenomenon does not appear in the PI/Fe_3O_4 composite microspheres (Fig. 4b). Which illustrates that polyimide is well protected magnetite core from oxidation. Compared to the TGA curve of pure PI (Fig. 4c), the low decomposition temperature can be seen from the TGA curve of the PI/Fe_3O_4 composite microspheres. Which is possible due to magnetite cores have a catalytic action for PI decomposition. However, the temperature corresponding to the 5 % weight loss is 370 °C, as can be seen from the curve for PI/Fe_3O_4, which demonstrates that the PI/Fe_3O_4 composite microspheres have excellent thermal stability compared to composite microspheres coated with other polymers [31]. Compared to the TGA curve of the PI powder, we can observe 40 % of the mass retention in the curve of the PI/Fe_3O_4 composite microspheres, which demonstrates that the PI/Fe_3O_4 composite microspheres have 60 wt% polyimide loading.

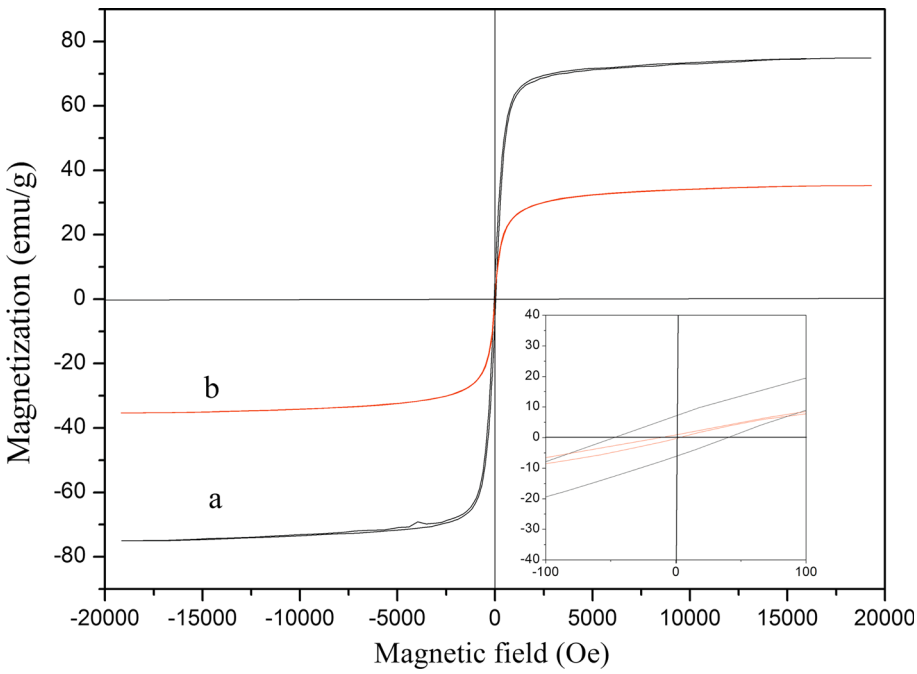

Fig. 6 Magnetization curves of (*a*) pure Fe_3O_4 and (*b*) PI/Fe_3O_4 composite microspheres

The PI/Fe_3O_4 composite microspheres have magnetic properties to be manipulated can be observed using a simple magnet. The sample was dispersed in the deionized water, a solution of PI/Fe_3O_4 composite microspheres before (Fig. 5a) and after (Fig. 5b) application of magnetic field clearly displays this feature, the samples gathered on the side of magnet in the magnetic field. The magnetic hysteresis loops of the pure Fe_3O_4 and the PI/Fe_3O_4 composite microspheres are shown in Fig. 6. The saturation magnetization of the PI/Fe_3O_4 composite microspheres is 35.29 emu/g, it is lower than that of the pure Fe_3O_4 (74.93 emu/g). This phenomenon should be attributed to the none-magnetic polyimide and polyimide leads the crystalline properties of Fe_3O_4 be worse. PI coated Fe_3O_4 exhibits an excellent thermal stability, although the presence of the polyimide reduces the saturation magnetization value of the samples. And the coercivity of PI/Fe_3O_4 composite microspheres decreased to 7.20 Oe compared with pure Fe_3O_4 (43.67 Oe), due to the crystalline size of PI/Fe_3O_4 composite microspheres decreases.

4 Conclusions

In this paper, a facile one-step solvothermal method has been developed and used to prepare the PI/Fe_3O_4 composite microspheres from PAAS and iron(III) ion. The diameter of the obtained PI/Fe_3O_4 composite microspheres is about 1 μm.The surface of particles is coated by PI, which penetrates throughout the entire samples with the total PI content of 60 wt%. It is demonstrated the composite microspheres have excellent thermal stability with considerable amounts polyimide by TGA, and it should protected magnetite core from oxidation.

Acknowledgments This work was supported by Yorth Science Foundation of Heilongjiang Province, China (Grant No. QC2014C008), Science Foundation of Heilongjiang Academy of Sciences, China (Nos. 2014-YQ-01, 2015-YX-02 and 2015-YQ-08).

References

1. L.H. Reddy, J.L. Arias, J. Nicolas, P. Couvreur, Chem. Rev. **112**, 5818 (2012)
2. J.K. Choi, J. Lee, Y.B. Lee, J.H. Hong, I.S. Kim, Y.K. Park et al., Chem. Phys. Lett. **428**, 125 (2006)
3. L.S. Sundar, E.V. Ramana, M.K. Singh, A.C.M.D. Sousa, Chem. Phys. Lett. **554**, 236 (2012)
4. J.J. Wei, H.L. Tang, X.B. Liu, J. Mater. Sci.: Mater. Electron. **25**, 520 (2014)
5. P.P. Qiu, W. Li, B. Thokchom, B. Park, M.C. Cui, D.Y. Zhao et al., J. Mater. Chem. A **3**, 6492 (2015)
6. X.G. Liu, N.D. Wu, C.Y. Cui, N.N. Bia, Y.P. Sun, RSC Adv. **5**, 24016 (2015)
7. K. Jia, J.D. Zhang, X. Huang, X.B. Liu, Chem. Phys. Lett. **614**, 31 (2014)
8. W. Jiang, W.F. Wang, B.C. Pan, Q.X. Zhang, W.M. Zhang, L. Lv, ACS Appl. Mater. Interfaces **6**, 3421 (2014)
9. M.F. Shao, F.Y. Ning, J.W. Zhao, M. Wei, D.G. Evans, X. Duan, J. Am. Chem. Soc. **134**, 1071 (2012)
10. X.F. Zhang, S. Mansouri, L. Clime, H.Q. Ly, L.H. Yahi, T. Veres, J. Mater. Chem. **22**, 14450 (2012)
11. Y. Tian, B.B. Yu, X. Li, K. Li, J. Mater. Chem. **21**, 2476 (2011)
12. L.S. Xiao, J.T. Li, D.F. Brougham, E.K. Fox, N. Feliu, A. Bushmelev et al., ACS Nano **5**, 6315 (2011)
13. D. Amara, S. Margel, J. Mater. Chem. **22**, 9268 (2012)

14. L.S. Lin, Z.X. Cong, J.B. Cao, K.M. Ke, Q.L. Peng, J.H. Gao et al., ACS Nano **8**, 3876 (2014)
15. R. Fu, X.M. Jin, J.L. Liang, W.S. Zheng, J.Q. Zhuang, W.S. Yang, J. Mater. Chem. **21**, 15352 (2011)
16. Y.H. Deng, D.W. Qi, C.H. Deng, X.M. Zhang, D.Y. Zhao, J. Am. Chem. Soc. **130**, 28 (2008)
17. T. Chen, X.Q. Zhang, J. Qian, S.J. Li, X.H. Jia, H.J. Song, J. Mater. Sci.: Mater. Electron. **25**, 1381 (2014)
18. X.B. Zhang, H.W. Tong, S.M. Liu, G.P. Yong, Y.F. Guan, J. Mater. Chem. A **1**, 7488 (2013)
19. S.H. Xuan, Y.J. Wang, J.C. Yu, K.C.F. Leung, Langmuir **25**, 11835 (2009)
20. C. Wang, H. Xu, C. Liang, Y.M. Liu, Z.W. Li, G.B. Yang et al., ACS Nano **7**, 6782 (2013)
21. B. Xu, H.J. Dou, K. Tao, K. Sun, J. Ding, W.B. Shi et al., Langmuir **27**, 12134 (2011)
22. J.L. Arias, L.H. Reddy, P. Couvreur, J. Mater. Chem. **22**, 7622 (2012)
23. F. Lan, Y. Wu, H. Hu, L.Q. Xie, Z.W. Gu, RSC Adv. **3**, 1557 (2013)
24. A.H. Lu, E.L. Salabas, F. Schth, Angew. Chem. Int. Ed. **46**, 1222 (2007)
25. D. Taguchi, T. Manaka, M. Iwamoto, Chem. Phys. Lett. **449**, 138 (2007)
26. C.G. Liu, C.Y. Qu, D.Z. Wang, H. Feng, P. Liu, Y. Zhang, J. Mater. Sci.: Mater. Electron. **26**, 4005 (2015)
27. D.J. Liaw, K.L. Wang, Y.C. Huang, K.R. Lee, J.Y. Lai, C.S. Ha, Prog. Polym. Sci. **37**, 907 (2012)
28. L. Zhang, J.T. Wu, N. Sun, X.M. Zhang, L. Jiang, J. Mater. Chem. A **2**, 7666 (2014)
29. J. Gao, X. Ran, C. Shi, H. Cheng, Y. Su, Nanoscale **5**, 7026 (2013)
30. F. Chen, R. Liu, S. Xiao, M. Lin, Mater. Lett. **130**, 101 (2014)
31. J.L. Castello, M. Gallardo, M.A. Busquets, J. Estelrich, Colloids Surf. A: Physicochem. Eng. Asp. **468**, 151 (2015)